Available online at www.sciencedirect.com

ScienceDirect

Procedia Manufacturing 47 (2020) 261–267

Procedia MANUFACTURING

www.elsevier.com/locate/procedia

23rd International Conference on Material Forming (ESAFORM 2020)

New Hybrid Manufacturing Routes Combining Forging and Additive Manufacturing to Efficiently Produce High Performance Components from Ti-6Al-4V

Frank Meiners[a,*], Jörg Ihne[a], Pascal Jürgens[a], Susanne Hemes[b], Michael Mathes[b], Irina Sizova[c], Markus Bambach[c], Rebar Hama-Saleh[d], Andreas Weisheit[d]

[a]*OTTO FUCHS KG, Derschlager Straße 26, Meinerzhagen D-58540, Germany*
[b]*ACCESS e.V., Intzestraße 5, Aachen D-52072, Germany*
[c]*Chair of Mechanical Design and Manufacturing, Brandenburg University of Technology Cottbus-Senftenberg, Konrad-Wachsmann-Allee 17, Cottbus D-03046, Germany*
[d]*Fraunhofer Institute for Laser Technology – ILT, Steinbach Straße 15, Aachen D-52074, Germany*

* Corresponding author. Tel.: +49-2354-73637; fax: +49-2354-73309; *E-mail address:* frank.meiners@otto-fuchs.com

Abstract

High-performance components from titanium alloy Ti-6Al-4V are used in many industries, particularly in aerospace, but also in the automotive and medical market. Traditionally, such components are produced by hot forging and subsequent post processing. The multi-stage forging process requires several expensive dies and leads to components with a high material oversize. Therefore, costly machining operations with machining removal up to more than 90% are necessary to produce the final geometry. This, in turn leads to a poor buy to fly ratio. New technologies, such as additive manufacturing (AM), could support traditional process chains and could enable a more resource-efficient production. However, in additive manufacturing production cycles are still long and manufacturing costs are very high, especially for larger parts. Thus, the production by AM is often limited to low quantities and smaller components. To overcome the above-mentioned disadvantages the present study proposes a hybrid manufacturing route, combining the advantages of forging and AM. The new manufacturing route could reduce the number of processing steps and forging dies, and additionally could provide efficient near-net-shape production. The presented route is based on a conventionally pre-formed forging, which does not yet have all the features of the final component. These features, such as ribs or other structural or functional geometries, will be added by additive manufacturing. The present study investigates the use of powder laser metal deposition (p-LMD) and wire-arc additive manufacturing (WAAM) for hybrid manufacturing of Ti-6Al-4V aerospace forgings.

Keywords: Hybrid Manufacturing; Forging; Additive Manufacturing; LMD; WAAM; Ti-6Al-4V

1. Introduction

The production of titanium-based high strength and temperature resistant components is of great importance for the transport and energy industry, and especially for the aerospace industry [1]. Usually these components are produced by hot forging operations. Mainly structural components for the aerospace industry are often characterized by an unfavorable cross-section and mass distribution for the forging process. Combined with the limited formability and the high resistance to deformation of titanium materials, this, on the one hand leads to multi-stage forging processes with expensive dies and, on the other hand to components with very high allowances for the finishing operations. Thus, the outstanding properties of a forged component are offset by high tooling costs, an extensive

10.1016/j.promfg.2020.04.215

process and low resource-efficiency, with a material yield far from 100% [2, 3].

For many applications, near-net-shape technologies such as additive manufacturing (AM) could enable a more resource-efficient production than conventional manufacturing routes [4]. However, process time and hence manufacturing costs in additive manufacturing rise rapidly with the part size [5]. Therefore, applying AM processes only partially could compensate for the lack of resource efficiency and flexibility of die-based serial production by forging.

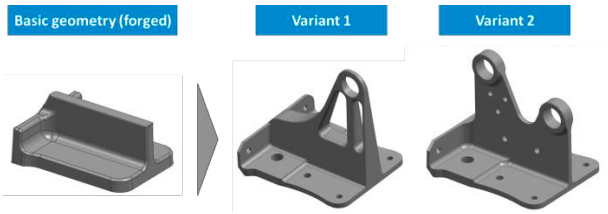

Fig. 1. Illustration of the hybrid manufacturing process route starting from a basic forged geometry followed by AM.

Combining AM and forging, two possible manufacturing routes can be put into practice:

First, an additive manufacturing process can be used to add structural or functional elements to a forged pre-form (see Fig. 1). This hybrid manufacturing route is currently subjected to intensive research [6-8]. However, most of the existing work on titanium alloy Ti-6Al-4V focuses on additive manufacturing of features for pre-formed sheet metal components. This study investigates the use of AM for generating or modifying ribs from Ti-6Al-4V on pre-forms created by hot forging, allowing for:

- simple creation of variants
- complex and near-net-shape components
- repair of parts
- local properties

The second manufacturing route can be used to generate a pre-form by AM, which then will be forged into its final shape by using only one single forging step. This innovative idea has been patented recently with a focus on titanium alloys [9, 10]. Moreover, previous studies of some of the authors of this paper showed that AM material provides good formability as well as lower flow stresses and activation energies for hot forming, compared to conventional wrought material with a lamellar microstructure usually used in conventional forging of titanium alloy Ti-6Al-4V [11, 12].

The present study investigates the use of two different additive manufacturing processes for hybrid manufacturing of Ti-6Al-4V high-performance aerospace components: i.e. powder laser metal deposition (p-LMD) and wire-arc additive manufacturing (WAAM).

Powder laser metal deposition is used to manufacture specimens for a fundamental analysis of the process as well as the behavior and properties of the specimens under different heat treatment conditions. After the basic characterization of specimens, a hybrid bracket as shown in Fig. 1, is manufactured by p-LMD and by wire-arc additive manufacturing. The WAAM process seems to be superior to other AM techniques – such as p-LMD – regarding the manufacturing time and deposition rate, power efficiency as well as investment costs [13].

The paper is structured as follows: Section 2 gives a deep overview of the manufacturing of the specimens considered in this study. Also, the procedures used for microstructural analysis and for the determination of mechanical properties are presented. Section 3 details the results and discussion of the manufactured and analyzed specimens. The microstructure and mechanical properties are presented and discussed. Section 4 shows an example for the hybrid manufacturing route forging followed by AM. A hybrid bracket from alloy Ti-6Al-4V is manufactured by p-LMD and WAAM. Finally, section 5 deals with the conclusions and an outlook.

2. Materials and methods

2.1. Manufacturing of specimens by powder laser metal deposition

Laser metal deposition is an additive manufacturing process with the ability to generate complex 3D parts. In the powder-based laser metal deposition, the powder material is deposited on a substrate by means of a laser beam. The powder is fed coaxially via a powder feed nozzle into the interaction zone of the laser beam and surface of the base material where it is completely melted. At the same time, a thin edge layer is melted. After solidification, a dense and metallurgically bonded track is formed on the substrate (see Fig. 2). Layer-by-layer deposition enables the manufacturing of 3-dimensional parts [14].

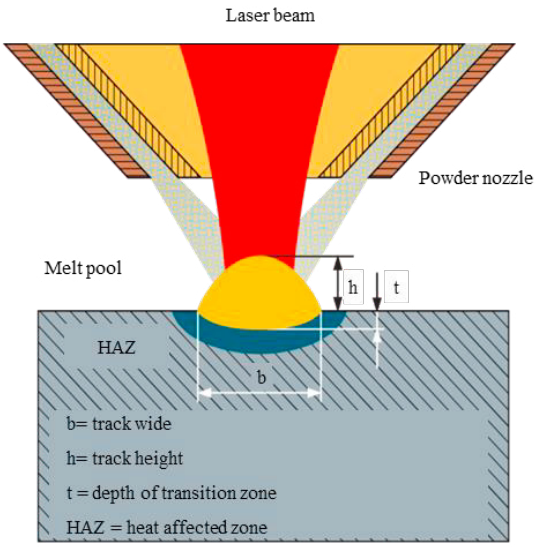

Fig. 2. Scheme of powder laser metal deposition (p-LMD).

A handling system with three axes is used to carry out the experiments. A diode laser with a maximum output power of 12 kW is used. The emitted wavelengths are 940 nm, 980 nm, 1030 nm and 1060 nm. The laser beam is guided into the optic via an optical fiber. The optic consists of a collimation and

motor-driven focusing lenses, acting as a zoom. With this zoom-optic, spot diameters between 3 to 9 mm can be realized. The powder (grain size 45 to 90 µm) is carried in an inert gas stream from the powder feeder, via tubes into the nozzle, forming a ring-shaped powder gas stream which is finally fed into the melt pool, generated by the laser beam. While the carrier-gas is suitable to protect the melt pool from oxidation, in addition, the whole part must be protected by an inert gas atmosphere. The set-up used is shown in Fig. 3.

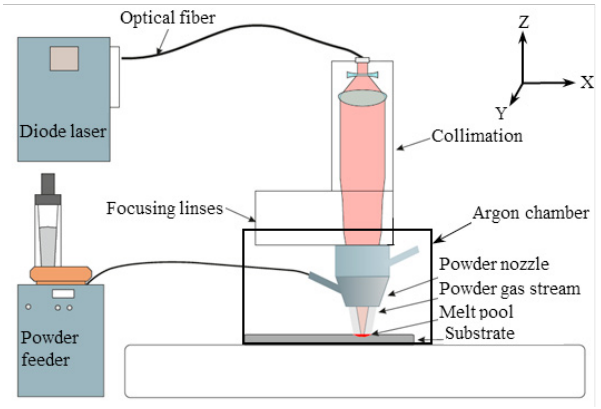

Fig. 3. LMD set-up with laser beam source, powder feeder, optic, powder feed nozzle and inert gas chamber [14].

To produce the three-dimensional specimens considered in this study (see Fig. 4) the build-up strategy is adapted to the geometry in a way that the start and end points of the single tracks do not significantly change the nominal geometry. To achieve this, the starting point of each layer is shifted by 90° and a contouring is added after each layer to ensure near-net-shape and edge stability during build-up. This strategy avoids accumulation of deposited material due to delay during laser on/off and acceleration/deceleration of the axes, since the powder is continuously fed.

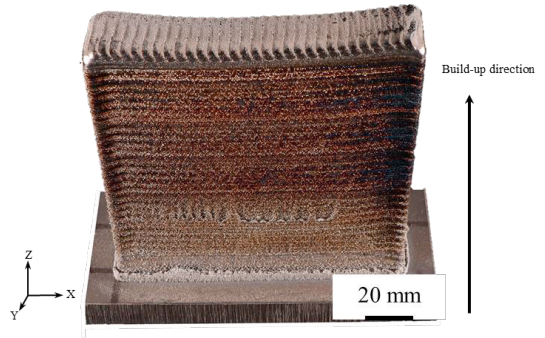

Fig. 4. Specimen produced by p-LMD from Ti-6Al-4V on a base plate with a geometry of the deposited material of 20 x 100 x 100 mm^3.

The process parameters used to build up the specimens for the fundamental analysis are shown in Table 1.

Table 1. Process parameters used for the p-LMD process.

Parameters	
Velocity	1500 mm/min
Laser power	1650 W
Powder mass flow rate	8.5 g/min
Laser spot diameter	3 mm
Deposition rate	0.5 kg/h
Shielding gas	Argon

2.2. Wire-arc additive manufacturing

To deposit the WAAM-layers on the forged basic geometry (see Fig. 1 and Fig. 10), wire with a diameter of 1 mm was fed into the melt pool produced by an electric arc, using a six-axis FANUC robot with a welding power source TPS/i 500 by Fronius. In order to prevent oxidation, the material was deposited within a closed argon gas chamber. The applied WAAM process parameters were the following: 95A current, 13V voltage, 8 m/min wire feed rate and the layer thickness was approximately 4 mm.

2.3. Heat treatments

To investigate the influence of different heat treatments on the microstructure evolution and mechanical properties, three different conditions were applied to the p-LMD material:

(1) “as-built”,
(2) stress-relief annealing at 710°C for 6h, followed by cooling at ambient air and
(3) β-annealing at 1050°C for 3h, followed by stress-relief annealing at 710°C for 6h, followed by cooling at ambient air.

2.4. Microstructural analysis

Prior to microstructural analyses, samples were cut from the specimens using wire-cutting, mounted with the cut cross-sections on top and ground flat with successively finer grades of silicon carbide papers from 320 to 1200 µm. Samples were then polished with 0.05 µm silica solution (Struers OP-S Suspension) with the addition of H_2O_2, HNO_3, and HF.

For microstructural analyses, different microscopes as well as a CT-scanner were used (i.e. Zeiss optical microscope Zeiss Imager.Z1m, equipped with an AxiaCAMHRc camera, HIROX digital microscope model MXG-2016Z and industrial CT Nikon, model METRIS/XTEK/XTH320LC). To obtain a resolution down to the nm range, as well as for the semi-quantitative elemental (EDX) and texture (EBSD) analysis, Zeiss Scanning Electron Microscopes (SEMs 1540XB, ULTRA55 and LEO1550), all equipped with Gemini columns, Oxford Instruments EDX-detectors (UltimMax170, X-MaxN150, and INCA X-act) as well as Oxford Tetra BSE-detectors and Nordlys EBSD-cameras were used.

To reconstruct the primary beta-grain-size from the measured alpha phase EBSD data, the Burgers orientation relationship (BOR), [15] and a modified approach after [16] and [17] were used.

2.5. Tensile testing

Tensile testing was performed at room temperature with a constant crosshead displacement rate. The round tensile specimens M10, had a dog-bone shape with a gauge length of 25 mm and a diameter of 5 mm. To estimate the impact of the build direction on the mechanical behavior, tensile specimens were extracted from the deposited material parallel (upright), transverse (lying) and at 45° to the build direction (see Fig. 5).

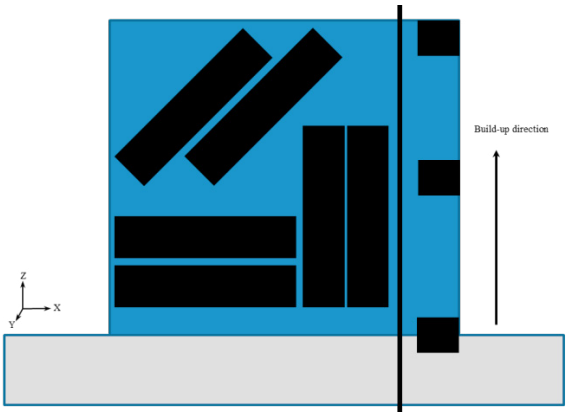

Fig. 5. Locations of extracted specimens

3. Results and discussion

3.1. Microstructure

Specimens were analyzed in their "as-built", stress-relief annealed and β-heat-treated states. The most important microstructural parameters are the thickness of the α-platelets, the grain size of the primary β-phase, as well as the existence of grain boundary α-phase (i.e. continuous α-phase at β-grain boundaries). Moreover, the homogeneity vs. heterogeneity of the microstructure and texture are of interest. Fig. 6 shows the microstructure of a Ti-6Al-4V specimen, manufactured by p-LMD, and the primary beta grain-size (a) as well as the single alpha-platelets (b) are indicated.

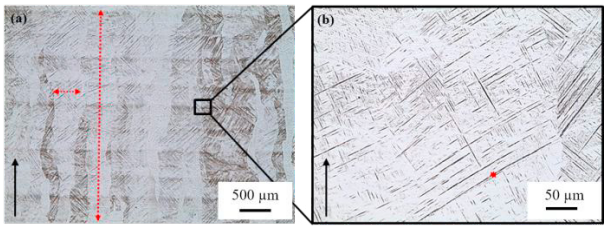

Fig 6. (a) Overview of starting microstructure of Ti-6Al-4V, manufactured by the p-LMD process; beta grain-width and length are indicated by red, dashed arrows. (b) Zoom-in, revealing single alpha-platelet-thickness (red arrow); whereas the build orientation is indicated by a thick black arrow.

As can be seen, p-LMD material shows a very fine-grained basket weave microstructure, with α-laths' thicknesses of about 0.94 µm (Fig. 6b). Moreover, the columnar prior beta-grains, with a width of about 250-500 µm, become obvious (Fig 6a). The development of such a fine-grained microstructure is the consequence of the rapid cooling during the p-LMD process. First the α-platelets form inside the primary β-grains, but are later-on transformed into a 'basket weave' microstructure, due to the exposure to heat transferred from the successively added adjacent layers. The primary β-grains tend to be elongated along the build-direction, due to the directional heat transfer during solidification, and the columnar grain-growth indicates the direction of cooling (i.e. the highest temperature gradient) during the p-LMD process.

Furthermore, as a result of the repeated re-melting of the material, during the addition of successive layers by p-LMD, as well as the overall heating-up of the material during the process, the primary beta grain-size tends to increase towards the top of the samples.

The average dimensions of the primary β-grains are about 3.5 mm parallel and ~ 300 µm transverse to the build direction (see Fig. 6a and Fig. 7a), with an overall sample size of ~ 20 x 100 x 100 mm^3. From a more detailed microstructural and textural (EBSD) analysis, grain boundary α-phase was found present on the primary β-grain boundaries (Fig. 7b). Moreover, the textural analysis shows the primary beta-grains to be preferentially oriented with their 100/001-axis parallel or slightly tilted from the build direction, which corresponds to the direction of cooling, or at least the maximum temperature gradient during p-LMD. The 'basket weave' α-phase inside the primary β-grains is randomly oriented (Fig. 7b).

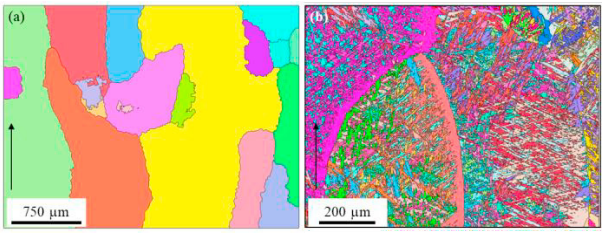

Fig. 7. Results of EBSD measurements of Ti-6Al-4V, manufactured by the p-LMD process; (a) reconstructed primary β-grains from the measured alpha-phase EBSD-data and (b) inverse pole figure (IPF-Z) map of the p-LMD material, showing grain boundary alpha. The build direction is indicated with an arrow.

Depending on the heat treatment, different macro- and microstructures can be produced in the p-LMD manufactured samples. Generally, stress-relieving treatments should decrease undesired residual stresses, resulting from the AM-process, without affecting the strength and/or the ductility of the samples.

Fig. 8 compares the macro- and microstructures of p-LMD manufactured material on forged base-plates, after different heat treatments. The macrostructures in the initial state ("as-built", see Fig. 8a) and after stress-relief annealing (Fig. 8b) appear to be very similar, with a primary beta grain width of ~ 200 µm and primary beta grains elongated in the direction of cooling. The microstructures however, differ from each other: whereas in the "as-built-state", close to the substrate, the microstructure can be described as fully martensitic, due to the rapid cooling, lacking any beta-phase matrix, in the stress-relief annealed sample, the microstructure consists of lamellar alpha-phase in a fine beta matrix. The thickness of the alpha-laths is

~ 1 µm in the "as-built" sample and ~ 1-2 µm in the stress-relief annealed specimens.

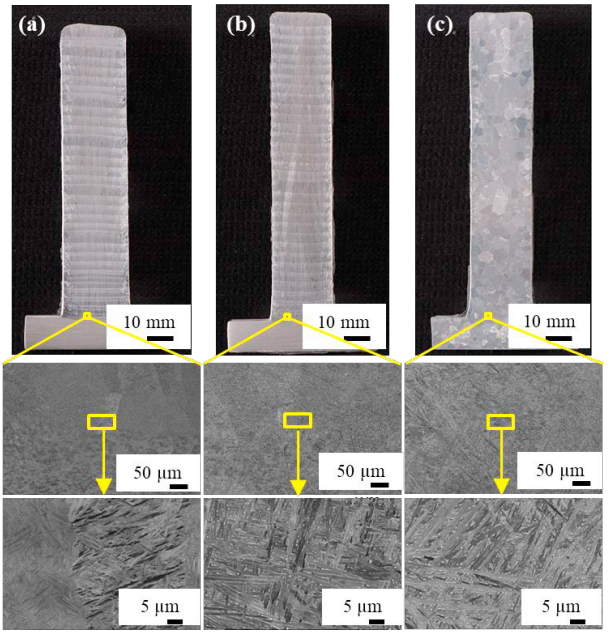

Fig. 8. Macro- and microstructures developed in "as-built" (a), stress-relief annealed (b) and β-heat-treated, followed by stress-relief-annealing (c) samples of Ti-6Al-4V p-LMD material.

During β-heat-treatment (Fig. 8c), the originally elongated β-grains are transformed into an equiaxed structure, due to the processing above the β-transus temperature, and thus lose their primary shape. To prevent excessive grain growth, the temperature for the β-annealing was selected only slightly higher than the β-transus temperature, still resulting in relatively coarse beta grains, with a size of ~ 1.2 mm in diameter. The microstructure of the beta-heat-treated sample is very similar to the stress-relief annealed sample and can again be described as a lamellar alpha-beta texture, consisting of fine α-laths of ~ 1-2 µm thickness within a fine beta matrix (see Fig. 8b and 8c).

3.2. Mechanical properties

The tensile test results for ultimate tensile strength (UTS), yield strength (YS) and elongation at break are summarized in Fig. 9. The given results were determined from two tensile specimens per heat treatment condition and sample orientation. For identical sample orientations, no systematic correlation was found between a sample's position and the result of its tensile test. However, there was a significant effect of sample orientation and heat treatment condition detected.

As mentioned above, the macrostructures of the "as-built" and stress-relieve annealed samples are very similar. As can be seen from Fig. 9, the tensile properties of these two sample conditions also show a similar trend. The strength is the highest for the 45° orientation and the lowest strength values were achieved for the parallel (0°) to the build direction orientation. While the strength difference between transverse (90°) and 45° is about 40 to 50 MPa, the strength of samples oriented parallel to the build direction decreases by an average of ~ 80 to 120 MPa. The tensile ductility however, was worse when measured in the transverse (90°) and 45° directions, compared to the direction parallel to the long axis of the primary β-grains. If the tests are carried out transversally to the prior β-grain boundaries, this is expected to promote premature failure through the grain-boundary α-phase, which also tends to be elongated along the build direction. This fact can also explain for the differences in ductility of the samples tested in the different orientations. Generally, by applying stress-relief annealing to p-LMD material, an increase of tensile ductility and a slight decrease of tensile strength was observed. This can be ascribed to the slight coarsening of α-platelets during stress-relief annealing (see Fig. 8), as well as to the reduced internal porosity of the material through re-sintering of some poorly bonded particles by heat treatment [18].

In case of the specimen subjected to β-heat-treatment, the anisotropy of tensile strength and ductility cannot be observed anymore. As mentioned above, heating above the β-transus temperature eliminates texture and changes the elongated prior β-grains into an equiaxed structure. However, the resulting coarse beta-grains as well as the lamellar α+β microstructure seem to decrease the tensile ductility to approximately 6-7 %.

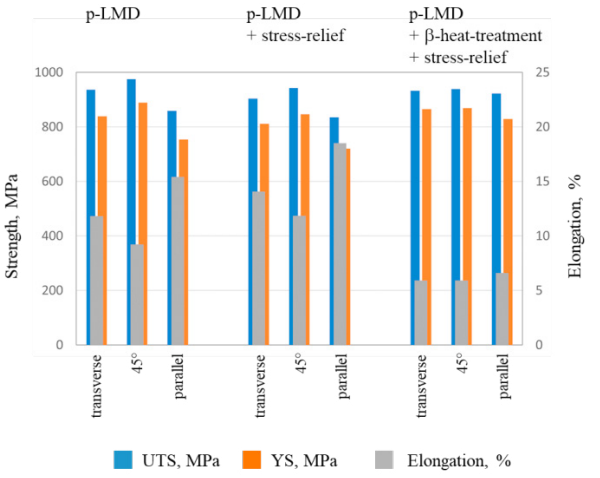

Fig. 9. Average results from tensile testing for different process conditions; p-LMD "as-built", p-LMD stress-relief annealed and p-LMD β-heat-treated + stress-relief annealed.

In summary, the found values of mechanical properties are comparable with literature data of additively manufactured tensile samples. The tensile properties of Ti-6Al-4V produced by AM are often comparable to cast or wrought material properties. The tensile properties obtained in the present study are comparable to the strength and ductility requirements of cast Ti-6Al-4V material, specified by ASTM B367 C5 and even of forged Ti-6Al-4V specified by ASTM B381 F5. Table 2 clearly shows that the requirements of ASTM B367 "Standard Specification for Titanium and Titanium Alloy Castings" are exceeded in all cases, if the beta-annealed samples are compared. When comparing stress-relief annealed specimens with the specification ASTM B381 "Standard Specification for Titanium and Titanium Alloy Forgings", the

specified requirements are not achieved for tensile and yield strengths at parallel orientation.

Table 2. Average results from tensile testing for different process conditions, compared to the requirements specified for cast ASTM B367 grade C5 and forged ASTM B381 grade F5 Ti-6Al-4V alloy.

	YS, MPa	UTS, MPa	Elongation, %
ASTM B381	825	895	10
stress relief annealing			
parallel to BD	87%	93%	190%
transverse to BD	98%	101%	140%
at 45° to BD	103%	105%	120%
ASTM B367	825	895	6
β-heat treatment + stress relief annealing			
parallel to BD	100%	103%	117%
transverse to BD	105%	105%	100%
at 45° to BD	105%	104%	100%

4. Production of a hybrid part

As shown in the previous section, the p-LMD process can be used to produce components made from Ti-6Al-4V with a tensile strength and ductility almost comparable to the strength requirements of conventionally processed Ti-6Al-4V material. Hence, the developed technique was applied to the production of a hybrid bracket.

In addition, wire-arc additive manufacturing was used to further accelerate the production and to manufacture the same component. As base material, a forged T-section from titanium alloy Ti-6Al-4V was used. Fig. 10 shows the forged base material and two different geometries, manufactured by the two different AM-techniques, as well as a final machined part.

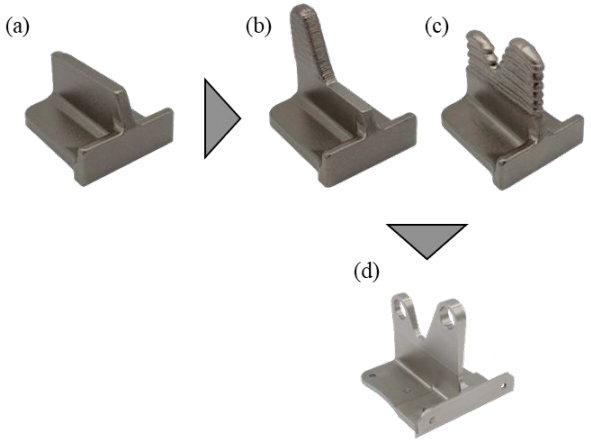

Fig. 10. (a) forged T-section, (b) forged T-section with added p-LMD structure, (c) forged T-section with added WAAM structure and (d) final machined hybrid Ti-6Al-4V part.

Applying p-LMD, various structures were deposited onto the forged T-section. The toolpath planning was carried out using the LMDCAM software developed at Fraunhofer ILT. For such a complex geometry, parameters like track-offset, distance between contour and hatch, and the build-up strategy can easily be set in the software. Machine data can be generated from the CAD file with the aid of a postprocessor (Fig. 11).

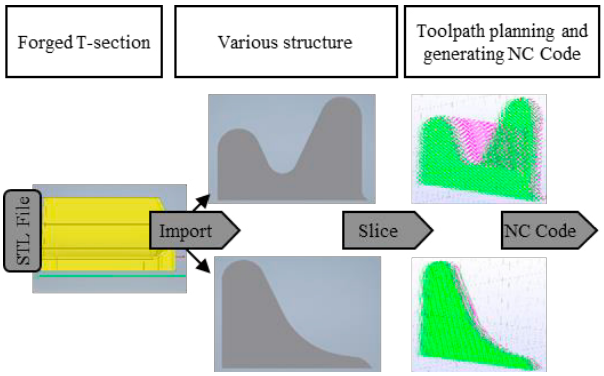

Fig. 11. Toolpath planning via LMDCAM from CAD file to NC Code.

For preparation, the forged T-section is milled on the top surface where the feature is added. The process duration varies according to the added geometry and volume. Subsequently, the final machining is carried out by milling the entire part. A deposition rate of 0.5 kg/h was achieved with a spot diameter of 3 mm. The oxygen content in the argon chamber is kept below 120 ppm during the process. Thus, the oxygen content in the AM material is only 0.11 wt. %.

At this point, the possibility of using wire-arc additive manufacturing to produce hybrid parts with near-net-shape geometry, was considered additionally, to be able to further enhance the deposition rate.

While p-LMD causes low heat input and allows for filigree structures, WAAM is characterized by high deposition rates of up to 10 kg/h [19] and thus surpasses other AM-techniques regarding process time and hence manufacturing costs.

In conclusion, using hybrid (forging + AM) technologies, material efficiency can be improved by about 50 % and technological limits from conventional hot-forging can be overcome.

5. Conclusions

In the present study, it was shown that powder laser metal deposition (p-LMD) can be used to produce hybrid aerospace components made from Ti-6Al-4V. It was demonstrated, that the microstructure and tensile properties can be adapted by applying different heat treatments. By doing so, specimens produced by p-LMD showed good tensile properties, which in many cases exceeded the requirements for conventionally processed material. In summary, the present study confirms that combining forging and AM, especially powder laser metal deposition and wire-arc additive manufacturing (WAAM), is a very promising manufacturing route to produce hybrid aerospace components made from Ti-6Al-4V. In particular, for larger-scale structural components, which are difficult to produce by forging and/or additive manufacturing alone, it would be very interesting to apply this hybrid manufacturing route.

Further optimization along the entire process chain will be required to realize the technological and economical potential of the presented hybrid process route, including investigations on the manufacturing route: AM followed by forging, as well as more detailed characterizations of other AM-processes, such as e.g. WAAM.

Acknowledgements

The authors gratefully acknowledge the financial support by the Federal Ministry for Economic Affairs and Energy (BMWi) for the LuFo project SAMT64 “Forging and additive manufacturing as a process combination for the resource-efficient production of aerospace structural components made of Ti-6Al-4V on flexible production scales”.

References

[1] Boyer RR. An overview on the use of titanium in the aerospace industry. Mater. Sci. Eng.: A 1996;213:103-114.

[2] Dutta B, Froes FH. Additive manufacturing of titanium alloys. Kidlington, Oxford: Butterworth-Heinemann; 2016.

[3] Liu S, Shin YC. Additive manufacturing of Ti6Al4V alloy: A review. Mater. Des. 2019;164:107552.

[4] Gibson I, Rosen D, Strucker B. Additive manufacturing technologies: 3D printing, rapid prottyping and direct digital manufacturing; Springer New York; 2014. p. 1-18.

[5] Liu Q, Wang Y, Zheng H, Tang K, Ding L, Li H, Gong S. Microstructure and mechanical properties of LMD-SLM hybrid forming of Ti6Al4V alloy. Mater. Sci. Eng.: A 2016;660:24-33.

[6] Bambach M, Sviridov A, Weisheit A, Schleifenbaum J. Case studies on local reinforcement of sheet metal components by laser additive manufacturing. Metals 2017;7:113.

[7] Merklein M, Dubjella P, Schaub A, Butzhammer L, Schmidt M. Interaction of additive manufacturing and forming. Proceedings of 6th international conference on additive technologies; 2016;309-316.

[8] Merklein M, Junker D, Schaub A, Neubauer F. Hybrid additive manufacturing technologies – an analysis regarding potentials and applications. Physics procedia 2016;83:549-559.

[9] Busch DM, Roegner EV, Colvin EL, Mueller LN, Rioja RJ, Bodily BH. Methods for producing forged products and other worked products, 2015, PCT/US2014/045952.

[10] Di DSE., Duperray L, Perrier F, Desrayaud C. Method for the production of parts made from metal or metal matrix composite and resulting from additive manufacturing followed by an operation involving the forging of said parts, 2015, PCT/FR2015/051087.

[11] Bambach M, Sizova I, Emdadi A. Development of a processing route for Ti-6Al-4V forgins based on preforms made by selective laser melting. J Manuf Processes 2019;37:150-158.

[12] Sizova I, Hirtler M, Günther M, Bambach M. Wire-arc additive manufacturing of preforms for forging of a Ti-6Al-4V turbine blade. AIP conference proceedings 2019;2113:150017.

[13] Bambach, M, Sizova, I, Sydow B, Hemes, S, Meiners, F. Hybrid Manufacturing of Components from Ti-6Al-4V by Metal Forming and Wire-Arc Additive Manufacturing. 1st International Conference on Advanced Joining Processes; 2019.

[14] Zhong, C. Process management, microstructure and mechanical properties in laser metal deposition of Inconel 718 with high deposition rates, Ergebnisse aus der Lasertechnik, 2019, Apprimus Verlag.

[15] Burgers WG. On the process of transition of the cubic-body-centered modification into the hexagonal-closed-packed modification of zirconium. Physica I 1934;36:561-586.

[16] Humbert M, Wagner F, Moustahfid H, Esling C. Determination of the orientation of a parent β grain from the orientations of the inherited α-plates in the phase transformation from body-centered cubic to hexagonal closed packed. J. Appl. Crystallogr. 1995;28:571-576.

[17] Simonelli M, Tse YY, Tuck C. On the texture formation of selective laser melted Ti-6Al-4V. Metall. Mater. Trans. A 2014;45:2863-2872.

[18] Xu Y, Lu Y, Sundberg KL, Liang J, Sisson RD. Effect of annealing treatments on the microstructure, mechanical properties and corrosion behavior of direct metal laser sintered Ti-6Al-4V. J. Mater. Eng. Perform. 2017;26:2572-2582.

[19] Williams, SW, Martina, F, Addison, AC, Ding, J, Pardal, G, Colegrove, P. Mater. Sci. Technol. 2015;32:641-647.